Available online at www.sciencedirect.com
ScienceDirect
International Journal of Pharmaceutics 329 (2007) 142–149
INTERNATIONAL JOURNAL OF PHARMACEUTICS
www.elsevier.com/locate/ijpharm

Pharmaceutical Nanotechnology

Formulation and characterization of amphotericin B–chitosan–dextran sulfate nanoparticles

Waree Tiyaboonchai [a,*], Nanteetip Limpeanchob [b]

[a] *Department of Pharmaceutical Technology, Naresuan University, Pitsanulok 65000, Thailand*
[b] *Department of Pharmacy Practice, Faculty of Pharmaceutical Science, Naresuan University, Pitsanulok 65000, Thailand*

Received 4 April 2006; received in revised form 9 August 2006; accepted 12 August 2006
Available online 17 August 2006

Abstract

A new nanoparticulate delivery system for amphotericin B (AmB) has been developed by means of the polyelectrolyte complexation technique. Two opposite charged polymers were used to form nanoparticles through electrostatic interaction, chitosan (CH) as a positively charged polymer and dextran sulfate (DS) as a polymer with a negative charge, together with zinc sulfate as a crosslinking and hardening agent. The AmB nanoparticles obtained possessed a mean particle size of 600–800 nm with a polydispersity index of 0.2, indicating a narrow size distribution. The measured zeta potential of the nanoparticle surface was approximately −32 mV indicating a strong negative charge at the particle's surface. Scanning electron microscopy revealed spherical particles with a smooth surface. Drug association efficacy of up to 65% was achieved. Dissolution studies demonstrated a fast release behavior suggesting that AmB exhibits only moderate interaction with the weakly crosslinked polymers of the nanoparticles. Although, electronic absorbance spectra showed that the aggregation state of AmB was modified within the nanoparticles, a reduction of nephrotoxicity was observed in an *in vivo* renal toxicity study.

Keywords: Amophotericin B; Chitosan; Dextran sulfate; Nanoparticles

1. Introduction

Amphotericin B (AmB) is a polyene macrolide antifungal agent and the drug of choice for systemic fungal infection. Unfortunately, it is poorly absorbed from the gastrointestinal tract due to its low aqueous solubility. Thus, it must be given parenterally to treat systemic fungal infections. Currently, two types of drug formulations for AmB are available. The first one is a micellar solution of AmB with deoxycholate as surfactant which may show serious nephrotoxicity. The second ones are lipid-based nanoparticulate formulations. These formulations have been found to reduce nephrotoxicity (Boswell et al., 1998), but are quite expensive. Thus, much effort has been spent to develop cheaper delivery systems with reduced amphotericin B toxicity. Recently, lower price amphotericin B disc formulations containing the cationic lipid dioctadecyldimethylamonium bromide have been developed. These formulations demonstrated some potential of lower nephrotoxicity but showed limited capacity of drug loading (Lincopan et al., 2005; Vieira and Carmona-Ribeiro, 2001). Polymeric nanoparticle delivery systems are one approach that has been extensively investigated (Espuelas et al., 2003; Sen et al., 1988; Venier-Julienne and Benoit, 1996).

There are a wide variety of techniques available for producing nanoparticles including solvent evaporation, interfacial polymerization and emulsion polymerization methods. Unfortunately, such processes frequently need the use of organic solvents or heat, which are undesirable process steps which may affect the integrity of the macrolide drug substance (Guerrero et al., 1998; Kreuter, 1988).

In contrast, coacervation is usually a simpler and milder encapsulation process than the above-mentioned methods (Burgess, 1990; Medan, 1978). This approach generally employs water-soluble polymers and is a straightforward method for the induction of the complex formation. Unfortunately, in many cases the coacervation method has to use glutaraldehyde or

* Corresponding author. Tel.: +66 55 261 000x3619; fax: +66 55 261 057.
E-mail address: wareet@nu.ac.th (W. Tiyaboonchai).

0378-5173/$ – see front matter © 2006 Elsevier B.V. All rights reserved.
doi:10.1016/j.ijpharm.2006.08.013

formaldehyde as a hardening agent which may cause toxicity. On the other hand, divalent ions as zinc ions can be used as a safe hardening agent through additional ionic interaction. Thus, in this study, we propose a new nanoparticle technique involving the self-assembly of polyelectrolytes, making use of the oppositely charged aqueous soluble polymers, chitosan (CH) and dextran sulfate (DS), with zinc sulfate as a stabilizing agent. Chitosan possesses many ideal properties of polymeric carriers for nanoparticles because it is biocompatible, biodegradable, nontoxic, and inexpensive. Chitosan is a modified natural carbohydrate polymer prepared by the partial *N*-deacetylation of chitin, a natural biopolymer derived from crustacean shells such as crabs, shrimps and lobsters. It is also found in some microorganisms, yeast and fungi.(Illum, 1998) The primary unit in the chitin polymer is 2-deoxy-2-(acetylamino) glucose. These units are combined by β-(l,4) glycosidic linkages, forming a long chain linear polymer. Although chitin is insoluble in most solvents, chitosan dissolves in most organic acidic solutions at pH less than 6.5 including formic, acetic, tartaric, and citric acid (LeHoux and Grondin, 1993; Peniston and Johnson, 1980).

Dextran sulfate is a biodegradable negatively charged polymer that is widely used for pharmaceutical applications. It has a branched chain of anhydroglucose units and contains approximately 17% sulfur, which is equivalent to approximately 2.3 sulfate groups per glucosyl residue.

The goal here was to characterize processing factors affecting the characteristics of CH–DS nanoparticles, including their physicochemical properties as well as the optimal conditions for their preparation. Size and morphology of nanoparticles were studied, as well as the efficiency of drug association and the mechanism of drug release. Moreover, the molecular structure of AmB which seems to be associated with its nephrotoxic properties in association with the nanoparticles was also investigated.

2. Materials and methods

2.1. Materials

Amphotericin B, dextran sulfate (MW 500,000), mannitol, and zinc sulfate were all purchased from Sigma Chemical (St. Louis, MO, USA). Chitosan (MW 30,000 with 95% deacetylation) was purchased from Aquapremier, Bangkok, Thailand. Fungizone® was the product of Bristol–Myers Squibb company (lot number A742). All other chemicals and solvents were of analytical grade. Cellulose ester dialysis membrane tubing with a molecular weight cutoff (MWCO) of 1,000,000 (Spectra/Por CE) was purchased from Fisher Scientific (Chicago, IL, USA).

2.2. Methods

2.2.1. Preparation of CS–DS nanoparticles and AmB loaded analogues

AmB containing nanoparticles were prepared by polyelectrolyte complexation at room temperature. Twenty microliters of an AmB in dimethylsulfoxide (DMSO) solution (10 mg/mL) were added to 0.075 mL of a DS aqueous solution (1%, w/v), mixed with 0.755 ml deionized (DI) water. The resulting solution was continuously stirred at 600 rpm. Then, 0.1 mL of aqueous chitosan solution (0.25%, w/v) was added drop-wise and the resulting nanoparticles were stirred for 5 min. Fifty microliters of a zinc sulfate solution (1 M) were then added. The resulting stabilized AmB nanoparticles were dialysed for 24 h in the dark against DI water using Spectra/Por CE MWCO 1,000,000 dialysing membrane. Then mannitol was added to the purified, loaded nanoparticles to a final concentration of 5% (w/v). The final suspension was then frozen and lyophilized (Dura-stop™, Dura Company, USA) at 0.4 mbar and −30 °C for 24 h. The lyophilized nanoparticles were stored in a desiccator at 4 °C. Mannitol was used as lyoprotectant and its concentration employed was based on results from previous work (Tiyaboonchai et al., 2001).

Nanoparticles were prepared with different processing parameters to study the effect of a number of variables on their physicochemical properties. Process parameters were varied as follows: the pH of a 0.25% (w/v) chitosan solution was varied from 3 to 5 and adjusted by the addition of 1.0 N NaOH solution; DS concentration was varied from 0.15 to 3.0 mg/mL and zinc sulfate from 12.5 to 75 μM; the CH to DS weight ratio was varied from 1:6 to 1:2. The ranges of these variable values were selected based on preliminary experiments. Empty nanoparticles were prepared using the same procedure. All samples were prepared in triplicate.

2.2.2. Physicochemical characterization of the nanoparticles

The morphology of both unloaded and AmB containing particles was investigated using scanning electron microscopy (1455VP, LEO Electron Microscopy Ltd., Cambridge, UK). The lyophilized particles were sprinkled onto a conductive sample holder and then sputter coated with a 20 nm gold–palladium (60:40) layer evaporator.

The mean particle size of the lyophilyzed nanoparticles was determined by dynamic light scattering (DLS) using a Brookhaven instrument (Holtsville, NY, USA). This instrument was fitted with a 50 mW HeNe diode laser operating at 532 nm (JDS Uniphase, San Jose, CA, USA), and a BI-200SM Goniometer with an EMI 9863 photomultiplier tube connected to a BI-9000AT digital correlator card. An aliquot of lyophilized particles was re-suspended in DI water. Measurements were then performed at 90° to the incident light and data were collected over a period of 3 min. The mean particle size and polydispersity index were obtained from the cumulative measurements (Koppel, 1972).

The zeta potential of the nanoparticles was determined by phase analysis light scattering employing a Zetasizer (Nano ZS90, Malvern, UK). The measurement angle was 90° to the incident light. Samples were prepared by re-dispersing 30 mg of lyophilized particles in 3.0 mL of DI water. Data were collected for 10 cycles. The zeta potential was calculated from the electrophoretic mobility using the Smoluchowski approximation approach (Tscharnuter et al., 1998).

2.2.3. Determination of drug association efficiency

Twelve milligrams of lyophilized nanoparticles were weighed and dissolved in 0.5 mL DMSO. This solution was centrifuged at 13,000 × *g* for 20 min and 30 μL of the supernatant was adjusted to 10 mL with methanol:water (1:1, v/v) solution. The amount of AmB was then determined spectrophotometrically at 408 nm. The percent drug association was then calculated according to the equation:

$$\text{Drug association (\%)} = \frac{\text{Amount of AmB in particle} \times \text{total particle mass} \times 100\%}{\text{Particle mass tested} \times \text{initial amount of AmB}} \quad (1)$$

2.2.4. In vitro dissolution studies

AmB possesses very poor aqueous solubility. In order to increase its solubility, 1% (v/v) Tween 80 in 10 mM HEPES buffer, pH 7.4, was used as a dissolution medium. The drug release profile of AmB nanoparticles was studied at 37 ± 0.5 °C. Nanoparticles containing 30 μg of AmB were placed into 20 mL of the dissolution medium and shaked in the dark. An aliquot (1 mL) was taken at predetermined time intervals of 5, 15, 30, and 60 min. The samples were filtered through a 0.2 μm membrane and the amount of AmB released was determined using HPLC method which was modified from Hosotsubo and Hosotsubo (1989). One hundred microliters of filtered sample, 500 μL of internal standard (0.5 μg/mL *p*-nitroaniline), and 400 μL of mobile phase were mixed. Fifty microliters of the mixture was then injected into the column. An HPLC apparatus (Thermo Separation Products, CA, USA) equipped with a 15 cm × 4.6 mm (i.d.) reversed-phase C18 column with a 5 μm particle size (Gemini Phenomenex, CA, USA) and UV–vis detector was used. The HPLC assay conditions were as follow: mobile phase: 10 mM acetate buffer, pH 7.2, and acetonitrile (63:37); flow rate: 1.2 mL/min; detection wavelength: 408 nm.

Dissolution studies were performed in triplicate. AmB content was determined by calculating the peak-height ratio of AmB to an internal standard.

2.2.5. Fourier transform infrared spectroscopy (FT-IR)

FT-IR spectra were obtained using a Spectrum GX series (Perkin-Elmer, MA, USA) equipped with a mirtgs detector and a extkbr beamsplitter. Spectra were obtained at 4 cm^{-1} resolution, under a dry air purge, and accumulation of 16 scans. The IR spectra of CH, DS and unloaded nanoparticles were obtained from the range of 4000–700 cm^{-1}. Spectra were obtained from KBr disc. The spectrum of the KBr disc was subtracted from each sample spectrum.

2.2.6. Characterization of AmB in nanoparticles using UV–vis spectroscopy

Lyophilized AmB nanoparticles were weighed and dispersed in 5.0 mL of DI water to give final AmB concentration of −10 μg/mL. The UV–vis spectra were obtained using an absorbance range from 300 to 450 nm. Unloaded nanoparticles were used as a blank.

2.2.7. In vivo determination of blood urea nitrogen and serum creatinine

Single dose injections in the tail vein of various doses of Fungizone® or AmB–CH nanoparticle formulation (equivalent to 1, 4, and 8 mg/kg amphotericin B) were given to groups of 5–8 male ICR mice, weighting 30–40 g. AmB–CH nanoparticles with a polymer (CH:DS) ratio of 1:3 was used in this study. Empty CH nanoparticles at equivalent amount of chitosan in AmB–CH nanoparticles were also injected into the mice as negative control. In order to investigate the effects of these formulations on the kidney function and toxicity, blood urea nitrogen (BUN) and serum creatinine were determined in the blood samples obtained from survivor mice at day 14. The data of each group of treated mice were compared with those of the control groups using one-way analysis of variance (ANOVA). Significant level was defined as $p < 0.05$.

3. Results

3.1. Physicochemical properties

3.1.1. Morphology

The morphology of lyophilized AmB loaded nanoparticles was examined by SEM. SEM micrographs of AmB loaded particles showed that the particles had a uniform spherical shape with a smooth surface and that they were uniformly distributed within the mannitol flakes (Fig. 1). Moreover, SEM micrographs of most formulations were similar indicating that processing conditions showed no or only little effect on the morphology of the nanoparticles.

3.1.2. Preparation parameters, mean particle size and size distribution

The prepared amphotericin B nanoparticle formulation was aimed for parenteral administration. Thus particle size and particle size distribution are crucial parameters for safe admin-

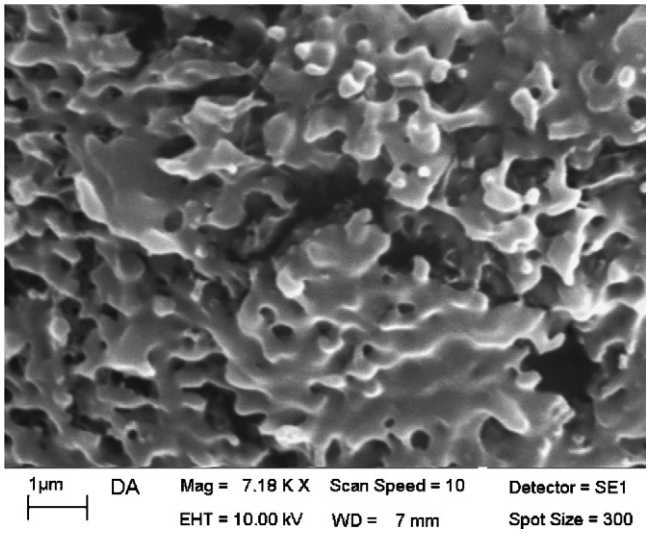

Fig. 1. SEM micrographs of lyophilized AmB loaded nanoparticles formed with pH 3 CH solution and a CH:DS mass ratio of 1:3 and lyophilized with 5% (w/v) mannitol.

Table 1
Effect of polymer ratio on the mean particle size and polydispersity of unloaded and AmB loaded particles

Polymer ratios (CH:DS)	Unloaded particles		AmB loaded particles	
	Mean (nm) ± S.D.	Polydispersity index	Mean (nm) ± S.D.	Polydispersity index
1:6	T	–	T	–
1:5	669 ± 330	0.22	644 ± 52	0.27
1:4	775 ± 181	0.26	630 ± 60	0.22
1:3	626 ± 107	0.27	721 ± 15	0.24
1:2	P	–	P	–

T, translucent system; P, precipitation which could not be measured by DLS. Preparation conditions: CH solution at pH 3 and 25 μM zinc sulfate.

istration of such a formulation. The mean particle size and size distribution of unloaded and AmB loaded nanoparticles were determined by dynamic light scattering. Visual observation and light scattering results showed that the pH of CH solution, the ratio of CH to DS, and polymer concentration were critical parameters in the nanoparticle formation.

The effect of the pH of CH solutions was studied by maintaining the polymer ratio at 1:3 while varying the pH of chitosan solution from 3 to 5. We found that the nanoparticles could be obtained only when formulated with pH 3 of the chitosan solution. Precipitation was observed when the coacervation process was done with chitosan solution of pH 4 and 5. One possibility may involve the charge intensity of CH. At lower pH, CH possesses a higher charge density and may act as protective colloid preventing particles precipitation. In the contrary, at higher pH values, CH has a lower charge density which may lead to particles aggregation through bridging flocculation. Recent literature has shown that there is also the possibility of direct sulfate adsorption onto the amphotericin B hydrophobic particle surface resulting in a reduced particle size and an improved colloidal stabilization of the amphotericin B dispersion (Mayer et al., 2005).

The effect of the polymer ratio was studied at pH 3 by using a fixed amount of the CH solution. The mean particles sizes were in the range of 600–720 nm with a polydispesity index of ∼0.2 when using CH:DS at a polymer ratio of 1:3 to 1:5 (Table 1). When the polymer ratio was greater than 1:5, the system became translucent suggesting that only a small amount of nanoparticles was obtained. At the same time, employing a polymer ratio smaller than 1:3, particle precipitation occurred. A similar result was observed when varying the amount of DS and additionally 25 μM zinc sulfate. The optimal amount of DS for nanoparticls formation was found to be in the range of 0.45–1.5 mg/mL (Table 2). Again, these formulations possessed a mean particle size in the range of 700–800 nm with polydispersity index ∼0.2. The mean particle size of AmB loaded particles was slightly higher than that one of unloaded nanoparticles.

From previous studied, we found that zinc sulfate was acting as a stabilizing agent by crosslinking the polymers additionally (Tiyaboonchai et al., 2001). Thus, the effect of zinc sulfate was investigated by maintaining the polymer mass ratio at 1:3 and employing a pH 3 of the CH solution while changing the amount of zinc sulfate. When increasing the amount of zinc sulfate, the mean particle size of unloaded nanoparticles tended to decrease suggesting that zinc sulfate may act as hardening agent (Table 3). The possible mechanism involved is the electrostatic interactions between zinc ions and the sulfate groups of DS on the particles surface. However the key components for the formation of nanoparticles are the two opposite charged polymers CH and DS. Moreover, as the amount of zinc sulfate exceeds this concentration, the mean particle size remains constant. In contrast, the mean particles size of AmB nanoparticles formulated with <25 and >25 μM zinc sulfate showed larger mean particle size than that formulated with 25 μM zinc sulfate. These results indicated that the optimal amount of zinc sulfate was 25 μM since this amount produced the smallest particle size and similar mean particle sizes of both unloaded and AmB loaded nanoparticles.

Zeta potential studies of the nanoparticles showed that there were no significant differences in the resulting zeta potentials when varying the processing parameters (data not shown). The zeta potential of all formulations was in the range of −27 until −37 mV suggesting free sulfate groups on the particles surface. Particles suspensions before dialysis possessed a pH of 3. Therefore, those nanoparticles will have less protonated sulfate groups available on their surfaces. When these particles were dialyzed against pH 7 DI water, the sulfate groups on the surfaces of

Table 2
Effect of dextran sulfate concentration on the mean particle size and polydispersity of unloaded and AmB loaded particles

Dextran sulfate (mg/mL)	Unloaded particles		AmB loaded particles	
	Mean (nm) ± S.D.	Polydispersity index	Mean (nm) ± S.D.	Polydispersity index
0.15	T	–	T	–
0.45	659 ± 128	0.30	771 ± 47	0.21
0.75	626 ± 107	0.27	721 ± 15	0.24
1.5	821 ± 262	0.28	807 ± 92	0.24
3	P	–	P	–

T, translucent system; P, precipitation which could not be measured by DLS. Preparation conditions: CH solution at pH 3, CH:DS mass ratio of 1:3, and 25 μM zinc sulfate.

Table 3
Effect of zinc sulfate concentration on the mean particle size and polydispersity of unloaded and AmB loaded particles

Zinc Sulfate (μM)	Unloaded particles		AmB loaded particles	
	Mean (nm) ± S.D.	Polydispersity index	Mean (nm) ± S.D.	Polydispersity index
12.5	717 ± 245	0.24	857 ± 466	0.26
25	626 ± 107	0.27	721 ± 15	0.24
37.5	638 ± 161	0.25	1040 ± 310	0.26
50	616 ± 132	0.22	999 ± 128	0.31
75	P	–	P	–

P, precipitation which could not be measured by DLS. Preparation conditions: CH solution at pH 3 and CH:DS mass ratio of 1:3.

particles presumably became more protonated which resulted in higher negative zeta potential values.

3.2. Determination of association efficacy

The association efficacy was done by dissolving AmB nanoparticles in DMSO and measured the amount of AmB using its absorbance at 408 nm. The results showed that most formulations demonstrated an association efficiency of 50–65% (Table 4). A small reduction in drug association was also seen when the nanoparticles were formulated with DS at a concentration of 1.5 mg/mL. This may be a result of competitive interaction between AmB and DS to interact with the positively charged CH.

3.3. In vitro dissolution studies

The percentage of cumulative AmB released from nanoparticles at varying time intervals in the dissolution medium, consisting of 1% (v/v) Tween 80 in HEPES buffer pH 7.4, at 37 °C was examined. A fast release characteristic of AmB was seen independent of the processing conditions with most of AmB released from particles within 5 min (data not shown).

3.4. FT-IR analysis

FT-IR spectra of DS showed sulfate asymmetric stretching absorption bands at 1244 and 1251 cm^{-1} (Cabassi et al., 1978) (Fig. 2A), while chitosan produced little IR absorption in this region (Fig. 2B). Thus, any changes in this region can be used to detect the interaction of the dextran sulfate groups in the nanoparticles. FT-IR analysis of CH showed an asymmetric NH bending absorption band at 1652 and 1599 cm^{-1}, respectively (Silverstein and Webster, 1998). When FT-IR spectra of CH–DS nanoparticles were examined, changes in the amine and sulfate absorption bands were detected (Fig. 2C). These spectral changes were attributed to the electrostatic interaction between the CH amine and DS sulfate groups. The asymmetric stretching of sulfate group in pure DS may produce a number of vibrations in the 1280–1200 cm^{-1} range resulting in a doublet peak of high intensity at 1244 and 1251 cm^{-1}, respectively. Electrostatic interaction with the CH amine groups appears to shift to these bands to 1263 cm^{-1}. An NH bending absorption band shifted from 1652 and 1599 to 1623 cm^{-1} was observed in the

Table 4
Percentage of drug recovery employing different amounts of dextran sulfate and zinc sulfate

Dexran sulfate (mg/mL)[a]	Percentage of drug entrapped	Zinc sulfate (mg/mL)[b]	Percentage of drug entrapped
0.45	55 ± 9	3.6	56 ± 13
0.75	57 ± 10	7.2	57 ± 10
1.5	47 ± 19	10.8	65 ± 9
		14.4	57 ± 25

[a] Preparation conditions: CH solution at pH 3, CH:DS mass ratio of 1:3, and $ZnSO_4$ 7.2 mg/mL.
[b] Preparation conditions: CH solution at pH 3, CH:DS mass ratio of 1:3, and DS 0.75 mg/mL.

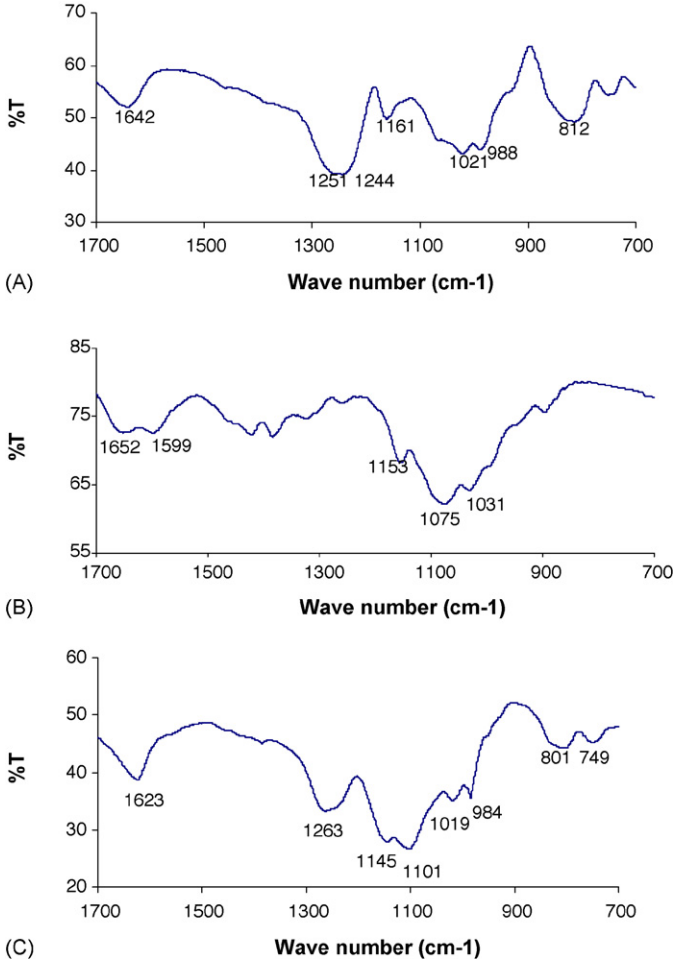

Fig. 2. IR spectra in the range of 1700–700 cm^{-1} of (A) DS, (B) CH, and (C) CH–DS nanoparticles.

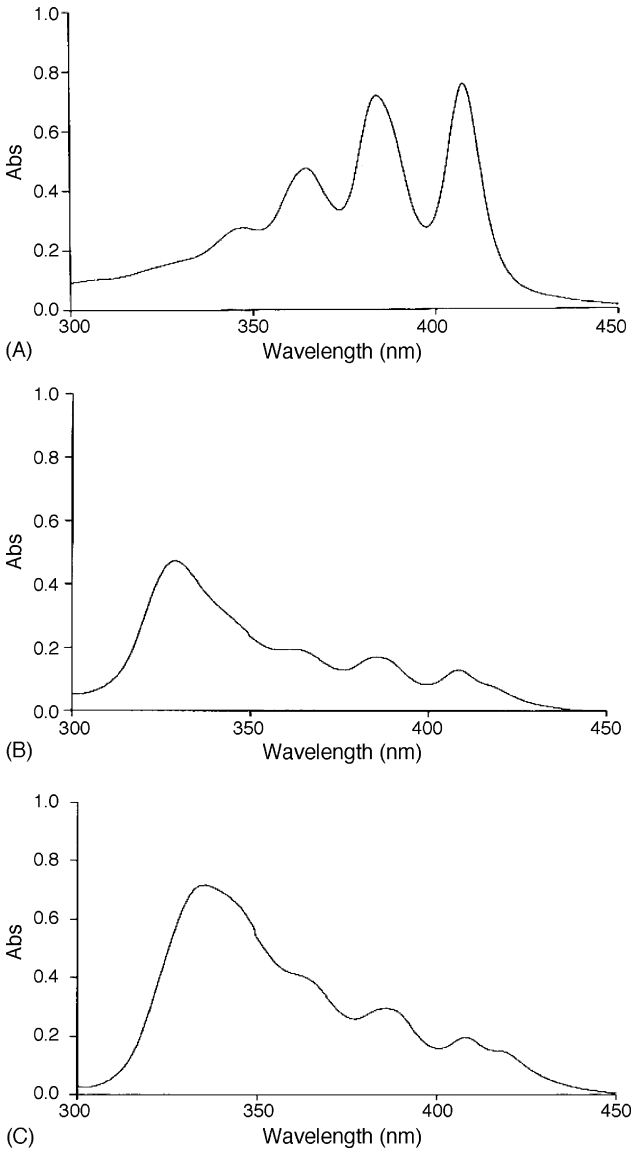

Fig. 3. Evolution of electronic absorbance spectra of ~10 μg/mL AmB in different formulation: (A) AmB in 50% methanol; (B) Fungizone® and (C) AmB nanoparticles prepared with pH 3 chitosan solution; CH:DS ratio of 1:3, and zinc sulfate of 25 μM.

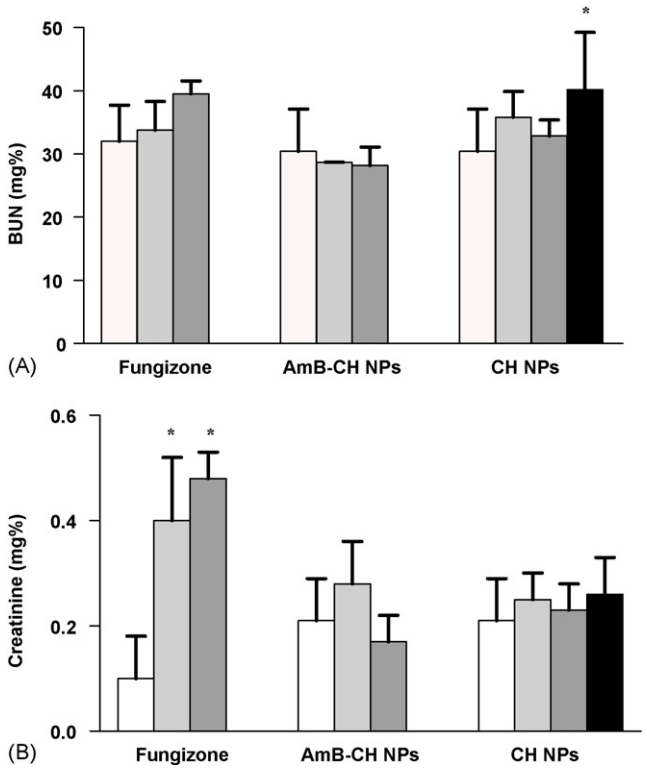

Fig. 4. Renal toxicity of Fungizone®, AmB–CH nanoparticles (NPs) and CH nanoparticles preapared with CH:DS of 1:3. The level of (A) serum BUN and (B) serum creatinine were detected in (□) control group, and in mice those treated with amphotericin B equivalent to (▒) 1 mg/kg, (▓) 4 mg/kg, and (■) 8 mg/kg. There is no survival from 8 mg/kg Fungizone® and AmB–CH nanoparticle ($^{*}p < 0.05$).

spectrum of the particles, also consistent with the presence of electrostatic interactions.

3.5. Characterization of AmB in nanoparticles using UV–vis spectroscopy

The UV–vis spectroscopy was used to investigate the aggregation state of AmB associated to the nanoparticles. The electronic absorbance spectrum of AmB in 50% (v/v) methanol, representing the monomeric form, showed high intensity peaks at 408, 384, and 364 nm and lower intensity peak at 345 nm (Fig. 3A). The absorbance spectrum of Fungizone®, which repesented the self-aggregation state of AmB, showed a broad peak with high intensity at 329 nm and less intense peaks at 365, 385, and 408 nm (Fig. 3B). The absorbance spectrum of AmB nanoparticles showed a similar shape as Fungizone® with a red shift from the peak 329–333 nm (Fig. 3C). The spectral changes due to self-aggregation of AmB can also be represented as the ratio of absorbance at the first peak (I) to the absorbance of fourth peak (IV). In a monomeric state, e.g., in 50% methanol solution, the I/IV ratio is about 0.37. The results showed that the I/IV ratio of Fungizone and AmB nanoparticles were 3.7 and 3.6, respectively.

3.6. In vivo determination of blood urea nitrogen and serum creatinine

To investigate the renal toxicity, mice were treated with normal to high dose of Fungizone® or AmB–CH nanoparticle formulations (equivalent to 1, 4, and 8 mg/kg amphotericin B). On the day 14, serum from survival mice was collected and analyzed for blood urea nitrogen (BUN) and creatinine levels (Fig. 4). Mice injected with all doses of Fungizone® had significantly increased serum creatinine concentrations. Although the serum BUN levels of these mice showed no statistical difference from the control group, there was a trend of increasing serum BUN values at a concentration of 4 mg/kg. This finding indicates a slight increase in renal toxicity after Fungizone® administration. On the contrary, serum BUN and creatinine levels of mice receiving AmB–CH or CH nanoparticles showed

no difference to the control group. However, serum BUN was found to be also significantly increased in mice receiving empty chitosan nanoparticles at the highest tested dose (∼7.2 mg/kg chitosan). It should be noted that the Fungizone® and AmB–CH nanoparticle experiments have to be conducted in different sets of animals; therefore the control levels were slightly different.

4. Discussion

CH–DS nanoparticles are formed by phase separation induced by electrostatic interactions between the positively and negatively charged polymers. They are formed rapidly when the two polymers are mixed together and interact with each other as recognized by solution turbidity. FT-IR spectra of CH–DS particles demonstrated spectral shifts in the sulfate and amine regions, confirming the existence of an electrostatic interaction between the sulfate groups of DS and the amine groups of CH.

In this work, the optimal conditions for formulating AmB nanoparticles in terms of their physicochemical properties were explored. The optimal conditions to obtain nanoparticles are the following; the ratio of CH:DS in the range of 1:3 to 1:5 (w/w); the dextran sulfate concentration in the range of 0.45–1.5 mg/mL; 25 μM Zinc sulfate; pH 3 of the CH solution. These experimental conditions result in the formation of nanoparticles in the range of 600–800 nm with a polydispesity index of 0.2 and a zetapotential of ∼32 mV. A drug association efficacy of up to 65% could be achieved.

In vitro dissolution studies in the presence of Tween 80 showed that this nanoparticle system provided rapid release of AmB suggesting that AmB was in its majority not incorporated into nanoparticles, but more likely adsorbed onto the particle surface. Nevertheless, AmB is insoluble in water, therefore, the release rate of AmB *in vivo* should be lower than that *in vitro* studied which may lead to slowly increasing AmB concentration in the plasma to avoid toxic effects.

The efficacy and the toxicity of amphotericin B are related to its aggregation state. The renal failure is believed to due to the aggregation of amphotericin B while monomeric form showed reduced renal toxicity (Barwicz et al., 1992). The molecular conformational changes of AmB, either due to self-aggregation or to its association with other compounds, can be detected by its absorbance using UV–vis spectroscopy. Thus, the molecular structure of AmB in nanoparticles was examined by its absorbance spectrum in the range of 300–450 nm. It is well known that AmB manifests two distinct electronic absorption spectra according to its molecular conformation. A spectrum of four well-separated bands at 344, 365, 385, and 410 nm was characterized as monomeric state of AmB. In contrast, a spectrum of broad single band at 328 accompanied by decreaseing in intensity at 365, 385, and 410 nm was characterized as aggregated state of AmB (Bolard et al., 1980; Rinnert et al., 1977).

The result showed that the spectrum of AmB nanoparticles were similar to that one of Fungizone® suggesting AmB in the aggregation state. However, slightly different spectra were found. The first peak of Fungizone® was at 329 nm indicating self-aggregation of AmB. On the contary, the spectrum of AmB nanoparticles showed a red shift of the 329 nm towards 333 nm. This spectral shift suggests that in the nanoparticles amphotericin B possesses a different aggregation state. The interaction between AmB and the nanoparticles was relatively weak as supported by the rapid release characteristic. Additionally, the degree of aggregation can be calculated using the ratio of absorbance at first peak (I), 333 nm, to the absorbance of the fourth peak (IV), 408 nm. The results showed that the I/IV ratio of Fungizone and AmB nanoparticles were 3.7 and 3.6, respectively, indicating that the aggregation state of amphotericin B in the nanoparticles is about the same as in Fungizone®.

The results show that AmB in AmB–CH nanoparticles as well as in Fungizone® formulations was predominantly present in the aggregated form. *In vivo* renal toxicity revealed that AmB–CH nanoparticles provided normal BUN and creatinine levels, while Fungizone® showed increased nephrotoxicity as an increase of creatinine was observed. The observed lower nephrotoxicity after administration of CH nanoparticles in comparison to Fungizone® may be due the fact that amphotericin B is slowlier released from the CH nanoparticles than from the deoxycholate micelles of Fungizone® resulting in sustained blood levels with the nanoparticulate formulation and to a quick high blood levels with the micellar formulation. This hypothesis has to be further investigated and substantiated. Chitosan when admisitered alone unexpectedly was found to also show some degree of renal toxicity due to the found increased BUN levels, however this effect was only observed at very high CH doses. It was previously demonstrated that low molecular weight chitosan was safe after intravenous administration (Richardson et al., 1999). However, further work has to be done to elucidate the effect of chitosans on the renal function.

In conclusion, the mean particles size of 600–800 nm could be successfully obtained by this technique. This nanoparticle system shows an attractive potential for the use as drug delivery system especially for heat or organic labile substances. Advantages of this technique are (1) ease of manufacturing and mild preparation condition, (2) use of biocompatible polymers, and (3) production in aqueous media avoiding organic solvents.

Acknowledgements

The author would like to thank Prof. Hans E. Junginger for his help in the manuscript preparation and discussion of the results. The author also thanks Premnapa Seesopa for her assistance in conducting the experiments. This study was supported by a grant from Naresuan University, Thailand.

References

Barwicz, J., Christian, S., Gruda, I., 1992. Effects of the aggregation state of amphotericin B on its toxicity to mice. Antimicrob. Agents Chemother. 36, 2310–2315.

Bolard, J., Seigneuret, M., Boudet, G., 1980. Interaction between phospholipid bilayer membranes and the polyene antibiotic amphotericin B: lipid state and cholesterol content dependence. Biochim. Biophys. Acta 599, 280–293.

Boswell, G.W., Buell, D., Bekersky, I., 1998. AmBisome (liposomal amphotericin B): a comparative review. J. Clin. Pharmacol. 38, 583–592.

Burgess, D.J., 1990. Practical analysis of complex coacervate systems. J. Colloid Interf. Sci. 140, 227–238.

Cabassi, F., Casu, B., Perlin, A., 1978. Infrared absorption and Raman scattering of sulfate groups of heparin and related glycosaminoglycans in aqueous solution. Carbohydr. Res. 63, 1–11.

Espuelas, M., Legrand, P., Campanero, M., Appel, M., Cheron, M., Gamazo, C., Barratt, G., Irache, J., 2003. Polymeric carriers for amphotericin B: in vitro activity, toxicity and therapeutic efficacy against systemic candidiasis in neutropenic mice. J. Antimicrob. Chemother. 52, 419–427.

Guerrero, D.Q., Allemann, E., Fessi, H., Doelker, E., 1998. Preparation techniques and mechanisms of formation of biodegradable nanoparticles from performed polymers. Drug Dev. Ind. Pharm. 24, 1113–1128.

Hosotsubo, H., Hosotsubo, K., 1989. Improved high-performance liquid chromatographic determination of amphotericin B in human serum and plasma. J. Pharm. Biomed. Anal. 7, 975–979.

Illum, L., 1998. Chitosan and its use as a pharmaceutical excipient. Pharm. Res. 15, 1326–1331.

Koppel, D.E., 1972. Analysis of macromolecular polydispersity in intensity correlation spectroscopy: the method of cumulants. J. Chem. Phys. 57, 4814–4820.

Kreuter, J., 1988. Nanoparticles. In: Swarbrick, J., Boylan, J.C. (Eds.), Encyclopedia of Pharmaceutical Technology. Marcel Dekker, New York, pp. 165–190.

LeHoux, J.G., Grondin, F., 1993. Some effects of chitosan on liver function in the rat. Endocrinology 132, 1078–1084.

Lincopan, N., Mamizuka, E., Carmona-Ribeiro, A., 2005. Low nephrotoxicity of an effective amphotericin B formulation with cationic bilayer fragments. J. Antimicrob. Chemother. 55, 727–734.

Mayer, G., Vogel, V., Weyermann, J., Lochmann, D., van den Broek, J., Tziatzios, C., Haase, W., Wouters, D., Schubert, U., Zimmer, A., et al., 2005. Oligonucleotide-protamine-albumin nanoparticles: protamine sulfate causes drastic size reduction. J. Control Release 106, 181–187.

Medan, P.L., 1978. Microencapsulation. I. Phase separation or coacervation. Drug Dev. Ind. Pharm. 4, 98–116.

Peniston, Q.P., Johnson, E., 1980. Process for the manufacturer of chitosan. US Patent 4,195,175, 25 March.

Richardson, S., Kolbe, H., Duncan, R., 1999. Potential of low molecular mass chitosan as a DNA delivery system: biocompatibility, body distribution and ability to complex and protect DNA. Int. J. Pharm. 173, 231–243.

Rinnert, H., Thirion, C., Dupont, G., Lematre, J., 1977. Structural studies on aqueous and hydroalcoholic solutions of a polyene antibiotic: amphotericin B. Biopolymers 16, 2419–2427.

Sen, N., Samanta, A., Baidya, S., Gupta, B., Ghosh, L., 1988. Development of amphotericin B loaded nanoparticles. Boll. Chim. Farm. 137, 295–297.

Silverstein, R.M., Webster, F.X., 1998. Infrared spectrometry. In: Spectrometric Identification of Organic Compounds, 6th ed. John Wiley & Sons Inc., New York, pp. 71–143.

Tiyaboonchai, W., Woiszwillo, J., Middaugh, C.R., 2001. Formulation and characterization of amphotericin B–polyethylenimine–dextran sulfate nanoparticles. J. Pharm. Sci. 90, 902–914.

Tscharnuter, W.W., Mcneil-Watson, F., Fairhurst, D., 1998. In: Provder, T. (Ed.), A New Instrument for the Measurement of Very Small Electrophoretic Mobilities Using Phase Analysis Light Scattering. American Chemical Society, pp. 327–340.

Venier-Julienne, M., Benoit, J., 1996. Preparation, purification and morphology of polymeric nanoparticles as drug carriers. Pharm. Acta Helv. 71, 121–128.

Vieira, D.B., Carmona-Ribeiro, A.M., 2001. Synthetic bilayer fragments for solubilization of amphotericin B. J. Colloid Interf. Sci. 244, 427–431.